

# International Conference on Space Optics—ICSO 2018

Chania, Greece

9–12 October 2018

*Edited by Zoran Sodnik, Nikos Karafolas, and Bruno Cugny*



## *Forward error correcting code for high data rate LEO satellite optical downlinks*

*S. Poulenard*

*B. Gadat*

*J. Chouteau*



ics0 proceedings



# Forward Error Correcting Code for High Data Rate LEO Satellite Optical Downlinks

S. Poulenard<sup>\*a</sup>, B. Gadat<sup>a</sup>, J.F. Chouteau<sup>a</sup>, T. Anfray<sup>a</sup>, C. Poulliat<sup>b</sup>, C. Jeco<sup>c</sup>, O. Hartmann<sup>c</sup>,  
G. Artaud<sup>d</sup>, H. Meric<sup>d</sup>

<sup>a</sup>Airbus Defence & Space, 31 rue des cosmonautes 31402 Toulouse; <sup>b</sup>CNRS IMS Laboratory, Bordeaux INP, University of Bordeaux, France; <sup>c</sup>ENSEEIH - Université de Toulouse, France ;  
<sup>d</sup>CNES, French Spatial Agency, Toulouse, France

## ABSTRACT

A simulation framework based on a physical-layer based abstraction to predict physical layer performances and to compare different forward error correcting (FEC) codes is presented. This framework is used to jointly design interleaving and FEC schemes for free space optical link. A sub-class of regular Low-Density Parity-Check codes is shown to be an interesting alternative to current space communication standard for optical links that require low error floor and high decoder throughput. End-to-end simulations show the feasibility of error free link from a LEO satellite to a high complexity ground station at 25Gbits/s and from a LEO satellite to low complexity optical ground station at 10 Gbits/s. The proposed protection scheme is composed of FG LDPC code and a bit interleaver to span the burst of errors.

**Keywords:** Optical link, error correcting code, LDPC code, decoder design

## 1. INTRODUCTION

Digital optical downlink at 1.55 $\mu$ m is foreseen to be a valuable alternative to the conventional radio-frequencies for the link between a LEO satellite and a fixed Earth ground station for missions such as Internet delivery and Earth observation data download. These two missions differ in terms of constraints and specifications leading to consider them separately. The current contribution considers two mission scenarii, on one hand a 10Gbps on-off-keying LEO downlink to a low complexity optical ground station, on the other hand a 25Gbps on-off-keying LEO downlink to a high complexity optical ground station. The low complexity refers to the O3K proposition at CCSDS with a receiver based on an avalanche photodiode (APD). The high complexity refers to the HDR proposition at CCSDS with a receiver based on an erbium doped fiber amplifier (EDFA) with a complex adaptive optic system to inject into its single mode fiber [1].

Since several years, the free space optical downlink community has investigated many different protection schemes: physical layer error correcting code combined with an interleaver [2][3], packet level erasure code [4][5], combination of all of them [6]. In the meantime, various FEC code families have been investigated: graph based codes (serial turbo code, or polar code [7], or sparse code such as Low Density Generator Matrix [3], Raptor [6], LT, Low-Density Parity-Check [9]), algebraic (MDS like Reed Salomon, BCH), and trellis based convolutional codes. Nevertheless, the comparison of these FEC codes with respect to frame error rate (FER) performances and hardware implementation complexity, particularly the decoder throughput and the power consumption, has not been deeply investigated to the author's knowledge. It results that system engineer might lack of data to select the "best" protection scheme and FEC code according to the specifications of the free space optical link they want to design.

The main idea is to propose a forward error correction scheme based on the combination of a physical layer error correcting code with a bit-interleaver to tradeoff FER performance, complexity and latency. The error correcting code shall have low error floor and enable high decoder throughput. In particular, we investigate on error correcting codes that have not been widely considered so far in the literature of space to ground optical downlink, ie. regular Finite Geometry Low-Density Parity-Check (FG LDPC) and Turbo Product Codes (TPC) [10] based on BCH. For comparison, we also consider other codes from the LDPC family such as Irregular Repeat Accumulate (IRA) codes, Accumulate Repeat Jagged Accumulate (ARJA) codes. The DVB-S2 LDPC codes are the reference scheme being a member of the latter [11].

The performances of the codes have been simulated on AFF3CT [15], an open-source software dedicated to FEC simulations. The optical transmission chains have been previously simulated on OptSim and by taking realistic sub-system parameters. The optical channel attenuations times series used for the sizing of the interleaver have been computed taking into account atmospheric propagation and realistic adaptive optic systems [12].

The paper is organized as follows: In section §2, we present the link budget of the two mission scenarii and the hypothesis made on the optical channel of propagation. In section §3, we present the two optical transmission chains and the resulting noise model. In section §4, we present the Frame Error Rate (FER) performances. Finally in section §5, the full chain is simulated and we provide examples of protection scheme addressing the 25Gbps on-off-keying LEO downlink to a high complexity optical ground station and also the 10Gbps on-off-keying LEO downlink to a low complexity optical ground station.

## 2. SCENARII FOR OPTICAL LEO DOWNLINK

The two scenarii are a 10Gbit/s On-Off-Keying (OOK) downlink from a LEO satellite at 500km to a low complexity Optical Ground Station (OGS) and a 25Gbit/s OOK downlink from a LEO satellite at 1200km to a high complexity OGS. These two scenarios differ on their transmitter on board the satellite, on their receivers on ground and on the impact of the atmospheric turbulence on the received optical power. The difference of optical transmitter and receiver leads to a difference of noise distribution and link budget. The difference of the impact of atmospheric turbulence leads to a difference of power fluctuation range and spectral content. For these reasons, the scenarii are considered separately.

### 2.1 Optical channel of propagation

The atmospheric turbulence is modelled by the Hufnagel-Valley profile [16] with an atmospheric turbulence level on ground of  $10^{-13}m^{-2/3}$  and a pseudo wind parameter of 21m/s. The wind is modelled by the Bufton model with an upper layer at 12 448m. The wind speed on ground is set to 10m/s and the upper layer wind speed is 25m/s. Such turbulence representation leads to Fried parameters at 1552nm on the Line of Sight (LoS) given in Table 1.

**Table 1: Fried parameter on LOS**

Elevation angle of LoS	[°]	10	20	30	40	60	80
Fried parameter on LoS at 1.55 $\mu$ m	[cm]	2,6	3,9	4,9	5,8	6,9	7,4

### 2.2 Scenarii description

For the 10Gbps OOK LEO downlink to a low complexity OGS, we consider a satellite at an altitude of 500km. The total transmitter power is 128.7dBm taking into account transmitter losses, antenna gain and optical amplifier power. The elevation angle of the line sight is 15°. On ground, the telescope diameter is 60cm and an adaptive optic system corrects the collected tip/tilt at a frequency of 1 kHz.

For the 25Gbps OOK LEO downlink to a high complexity OGS we consider a satellite at an altitude of 1200km. The total transmitter power is 130.9dBm taking into account transmitter losses, antenna gain and optical amplifier power. The elevation angle of the line sight is 20°. On ground, the telescope diameter is 60cm and an adaptive optic system corrects up to 12 radial orders at a frequency of 3 kHz [12].

**Table 2: Scenarii description**

		Low complexity 10Gbit/s OOK	High complexity 25Gbit/s OOK
Satellite orbit	[km]	500	1200
Elevation of the LoS	[°]	15	20
On ground telescope diameter	[cm]	60	60
Optical receiver type	[-]	APD multimode fiber	EDFA single mode fiber
Optical receiver diameter	[ $\mu$ m]	50	9
Radial order corrected by AO on-ground	[-]	1	12
Frequency of AO on-ground	[Hz]	1000	3000

The power available at the optical receiver without atmospheric turbulence losses and transmitter pointing error is computed in Table 3. The losses due to atmospheric turbulence and to transmitter pointing error are computed separately for the end-to-end simulation.

**Table 3: Link budget without turbulence losses and power losses due to on board optical terminal pointing error**

		Low complexity 10 Gbit/s OOK	High complexity 25Gbit/s OOK
<b>TOTAL transmitter</b>	[dBm]	<b>128,7</b>	<b>130,9</b>
Free space propagation	[dB]	-261,2	-266
Clouds impact	[dB]	-5,0	-5,0
Molecular absorption/diffusion	[dB]	-1,8	-1.3
<b>TOTAL channel</b>	[dB]	<b>-267,9</b>	<b>-272,3</b>
<b>TOTAL receiver</b>	[dB]	<b>119,0</b>	<b>119,0</b>
Implementation + system margin	[dB]	-3,0	-5,0
<b>Link budget w/o turbulence &amp; w/o pointing losses</b>	[dBm]	<b>-23,2</b>	<b>-27,4</b>

### 3. OPTICAL TRANSMISSION CHAIN CHARACTERISATION FOR FEC

The optical transmission chains are simulated with Optisim software taking into account datasheet parameters.

#### 3.1 Transmission chains

Figure 1 depicts the 25Gbits/s OOK high complexity transmission chain. At the transmitter, the laser is externally modulated with a Mach Zehnder Modulator (MZM). Then, an optical booster amplifier amplifies the signal and adds amplified autonomous noise. The channel block applies a static attenuation leading to a given Received Optical Power (ROP) at the input of the receiver based on a Low Noise Optical Amplifier (LNOA). At the PIN photodetection followed by a transimpedance amplifier(TIA), the signal is filtered by an electrical low pass filter (ELPF). The block BER computes the Bit Error Rate.

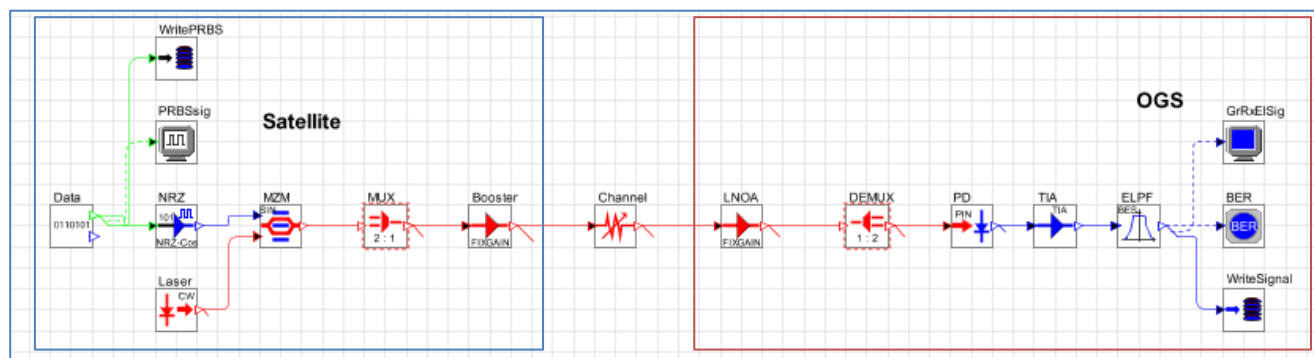


**Figure 1: 25Gbit/s OOK transmission chain - high complexity**

Figure 2 depicts the 10Gbit/s OOK low complexity transmission chain. At the transmitter side, the laser is directly modulated. Then, an optical booster amplifier amplifies the signal and adds amplified autonomous noise. The channel block applies a static attenuation leading to a given Received Optical Power (ROP) at the input of the receiver based on a multimode avalanche photodiode (APD). Background noise (BGNoise) is also considered in the transmission chain.

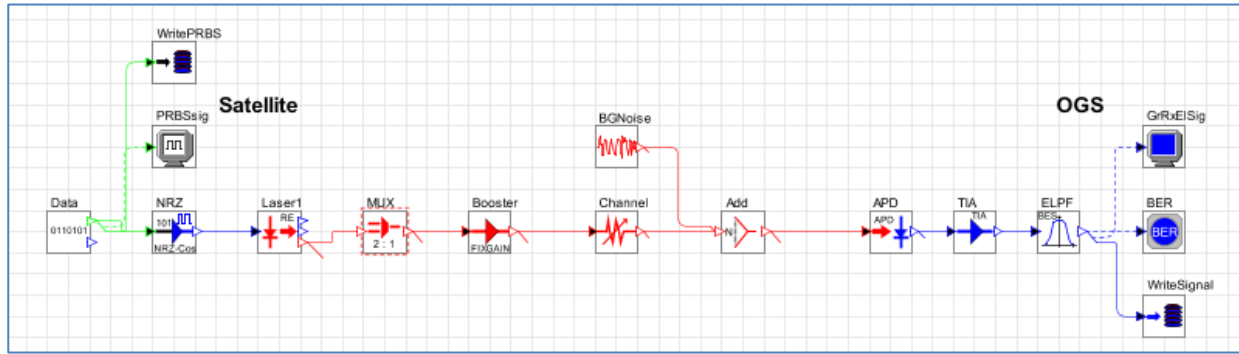


Figure 2: 10Gbit/s OOK transmission chain - low complexity

### 3.2 Noise model

Due to the inaccuracy of well-known noise contribution variances [13] to represent noisy signal distribution at the input of the decoder, we prefer to issue our noise model from Optsim simulation at bit level. For example, Figure 5 depicts the difference between Optsim and a MATLAB model implementing the formulas of [13] for the 25Gbit OOK high complexity transmission chain.

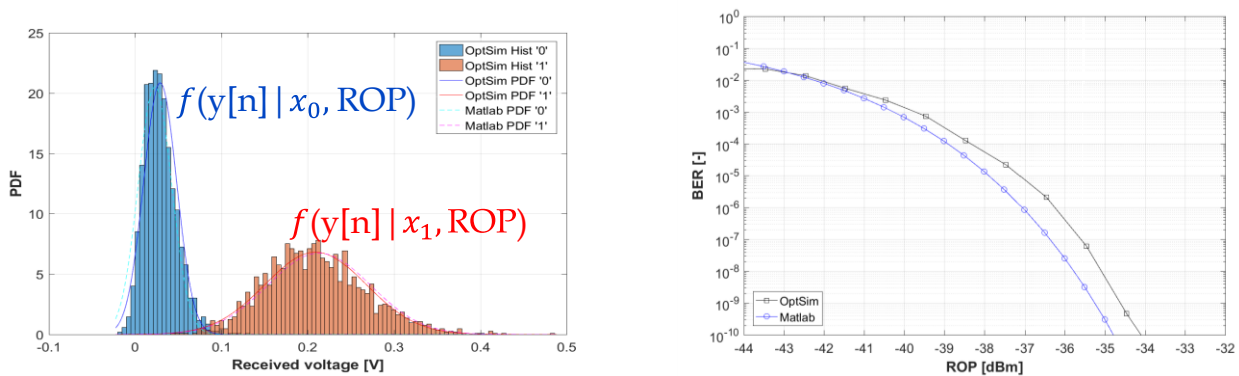


Figure 3: Comparison of the results between numerical simulation and analytical formulae in OOK for an EDFA based receiver (left) Probability Density Function of the noisy signal depending on the emitted bit '1' or '0' and the ROP (right) bit error rate function of the received optical power

### 3.3 Mutual information function of received optical power

Both transmission chains have been characterized with the mutual information [14] that measures the statistical correlation between two random variables, here the send code symbols and the received ones. In the present contribution the mutual information has been noted  $MI_{ECC}$  or  $MI$  and is computed according to formula (1) where  $x$  and  $y$  are respectively the signal sent by the transmitter and  $y$  the signal at the entry of the decoder, and  $p(x)$  and  $p(y)$  are the probability density functions.

$$MI_{ECC} = MI = \int_Y \int_X p(x,y) \cdot \log \left( \frac{p(x,y)}{p(x) \cdot p(y)} \right) dx dy \quad (1)$$

The mutual information is an interesting metric for FEC performances comparison as it enables to compare the FER performances of different systems operating on different channel conditions or channel models. It will be used to characterize the MI requirements for a FEC scheme to achieve a targeted FER after interleaving. The MI is also the maximum code rate achievable.

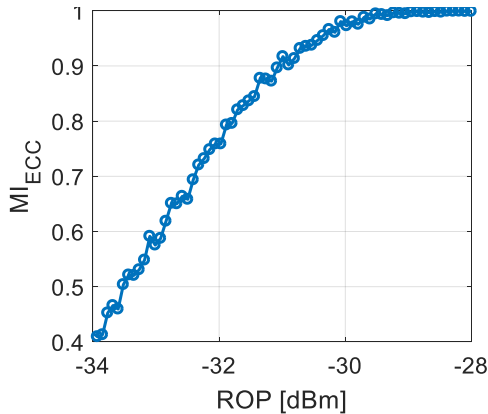


**Figure 4:  $MI_{ECC}$  function of received optical power - 10Gbit/s OOK – Low complexity**

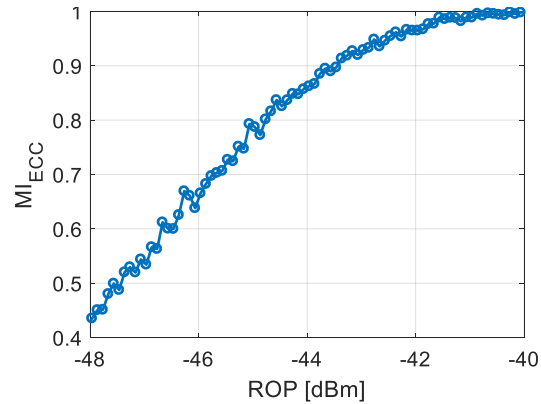


**Figure 5:  $MI_{ECC}$  function of received optical power - 25Gbit/s OOK – High complexity**

Figure 4 and Figure 5 depict the mutual information at the entry of the decoder  $MI_{ECC}$  function of the ROP at the input of the optical receiver. Figure 4 provides the result for the 10Gbit/s OOK low complexity chain based on an APD receiver. Figure 5 provided the result for the 25Gbit/s OOK high complexity chain based on an EDFA receiver.

#### 4. FRAME ERROR RATE PERFORMANCES OF ERROR CORRECTING CODES

New space optical links require high useful data rate, error free links and decoder friendly FEC codes. For this reason, we focused on FEC codes that enable to design decoder that can achieve high throughput such as Quasi-Cyclic LDPC codes [17] and Turbo Product Code.

##### 4.1 Considered FEC Codes

Quasi-Cyclic LDPC are a sub-class of structured codes that should achieve performances close to unstructured LDPC codes while being much more convenient for parallel encoder and decoder architecture design.

For the QC LDPC code family, we investigate:

- The Irregular Repeat Accumulate (IRA) codes constructed by Progressive-Edge-Growth (PEG) algorithm associated to an Approximated Cycle Extrinsic (ACE) constraint [18].
- The Accumulate Repeat Jagged Accumulate (ARJA) codes [18].
- The Finite Geometry (FG) codes [18].

For the DVB-S2 codes, we referred to the ETSI standard [11]. For the Turbo Product Code, BCH component codes are investigated.

In each case, the interleaving size and codes parameters, such length or size of circulants, are carefully selected both (a) to achieve a required FER after deinterleaving and (b) to enable full exploitation of byte-aligned hardware architecture.

Code rates of 1/2, 2/3, 4/5, 9/10 are considered but code rate superior or equal to 4/5 are more interesting to achieve high useful data rate. The code word length is around 16380 bits knowing that greater FEC frames would improve performances and enable higher decoder capacity for a given hardware.

##### 4.2 Decoding algorithm and its parameters

The LDPC codes (IRA, ARJA, FG) and the DVB-S2 codes are decoded thanks to the Normalized Min-Sum (NMS) algorithm [19] with a normalization factor of 0.75 and a number of decoding iteration limited to 10 iterations. This is a major difference with existing solutions: we should rather consider FEC schemes that enable rapid convergence rather than achieving the best threshold to enable high throughput decoders.

The TPC are decoded thanks to the Chase-Pyndiah decoder [10] with 32 test patterns and 8 iterations. The weighting factor  $\alpha(m) = [0.1 \ 0.1 \ 0.25 \ 0.25 \ 0.5 \ 0.5 \ 0.75 \ 0.75 \ \dots \ 1]$  and reliability factor  $\beta$  dynamically computed.

### 4.3 Performances

Figure 6 depicts the Frame Error Rate (FER) function of the Mutual Information (MI) seen at the entry of the decoder.

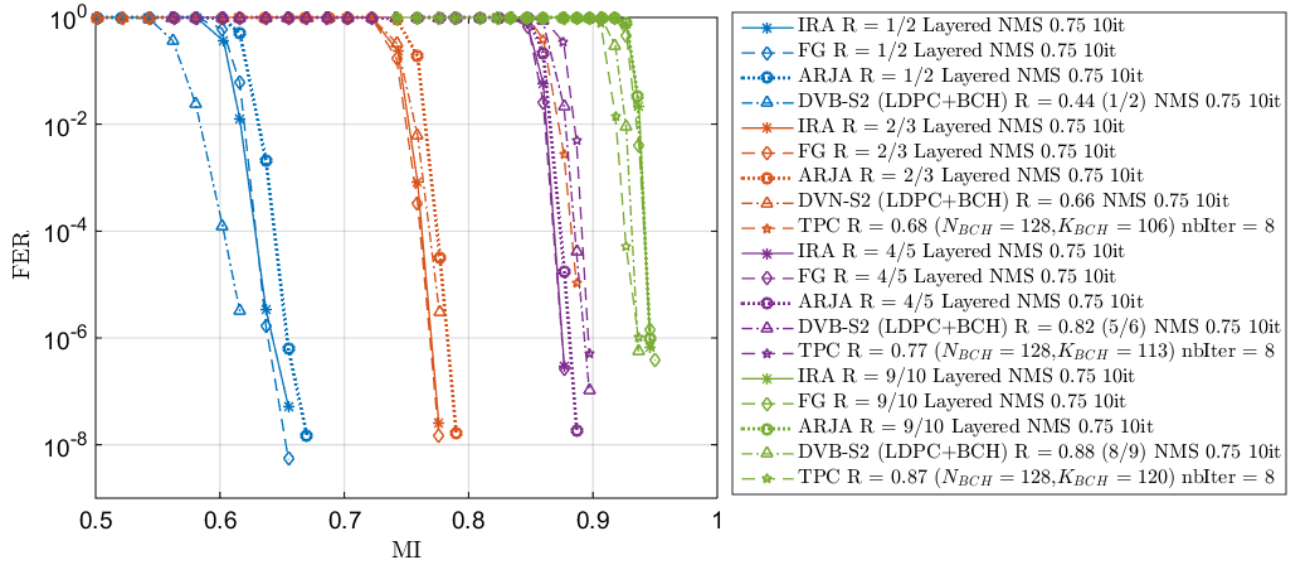


**Figure 6: Frame Error Rate function of the mutual information of the signal at the entry of the decoder. Blue, red, purple, green curves correspond respectively to code rate around 1/2, 2/3, 4/5, 9/10.**

It results that:

- For the QC LDPC family (IRA, ARJA, FG): The Finite Geometry sub-class provides better performances for low code rate and similar performances for high code rate. FG LDPC is more efficient than the IRA and ARJA in the study context.
- TPC based on BCH code component could be an interesting alternative for very high code rate, typically around 9/10.
- A strict comparison of performances between DVB-S2 (LDPC + BCH) codes and FG LDPC codes can be done for a code rate of 2/3. In this case, better performances are obtained with the FG LDPC code.

## 5. INTERLEAVER SIZING

In the previous section, we have shown that FG LDPC codes is an interesting FEC code for LEO downlink that requires high code rate, low error floor and high decoder throughput. In this section we present the simulation chain used to design the interleaver that is mandatory to span the burst of errors due to the slow fading optical channel.

### 5.1 Optical channel

We compute the Received Optical Power (ROP) time series by mixing the atmospheric turbulence attenuation time series computed by ONERA, the power losses time series due to transmitter pointing error computed by Airbus Defence and Space, and the link budget value presented in Table 3. Figure 8 depicts the characteristics of the power losses due to the on-board optical terminal pointing error and the power losses due to atmospheric turbulence considering adaptive optic system on ground. In our references scenarios, the losses due to the impacts of the atmospheric turbulence are predominant.

Note that these losses are slow compared to the optical data rate. As a result an interleaver is mandatory to span the burst of errors and to achieve quasi error free link thanks to the physical layer error correcting code.

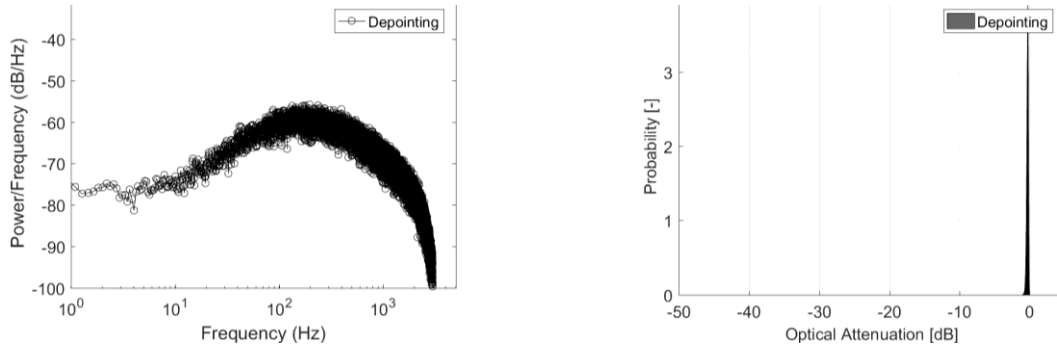


**Figure 7: Characteristic of power losses due to the on board optical terminal pointing error | (left) spectrogram, (right) distribution - high complexity scenario**

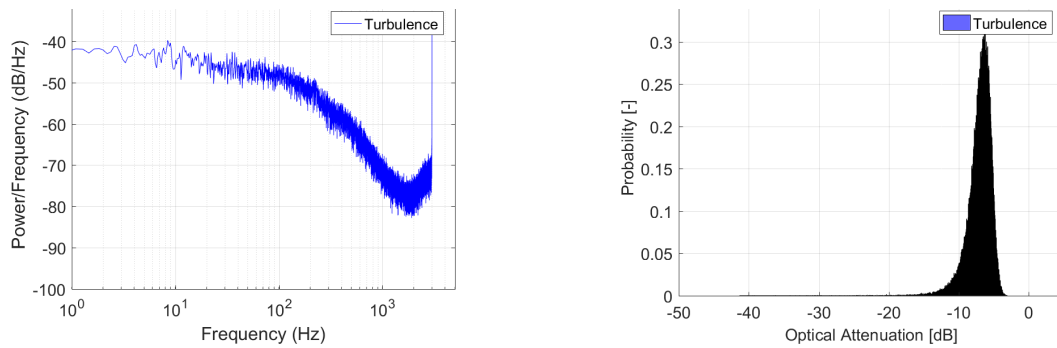


**Figure 8: Characteristic of power losses due to atmospheric turbulence considering adaptive optic system | (left) spectrogram, (right) distribution – high complexity scenario | ONERA time series**

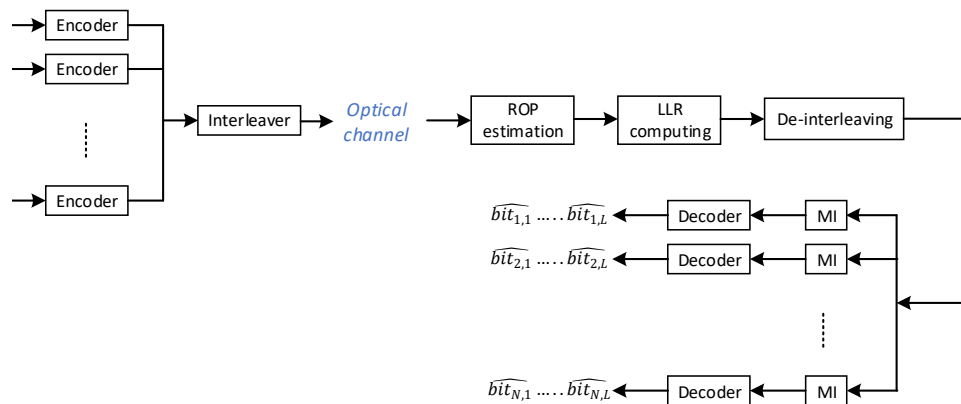
## 5.2 Interleaver sizing

Figure 9 depicts the simulation chain that has been designed to size the duration of the row column interleaver.

At the transmitter side, the bit generation, the encoder, and the row-column interleaver are joined. Then, the optical channel refers to the two steps:

1. To play the ROP time series available at the input of the optical receiver;
2. To convert the ROP and the emitted bit into a noisy signal corresponding to the signal available at the output of the optical receiver (see Figure 3).

Then the Log-likelihood ratios (LLRs) are computed under the assumption of equal probability of bit ‘0’, and ‘1’ before the de-interleaving process and the decoding process.



**Figure 9: Blocks of the simulation chain**



Table 4 provides the interleaver duration required for an error free link function of the FEC code rate. For both scenarios, according to simulations, a protection scheme composed of FG LDPC codes with a code rate of 4/5 and an interleaver of 10ms shall achieve error free communication at the considered elevation angles, respectively 15° for the low complexity downlink and 20° for the high complexity downlink.

As soon as the elevation angle increases, the link turns to be error free even before decoding as the link budget is overpowered.

In case the latency of the service is a hard constraint, the FEC code rate might be decrease.

**Table 4: Interleaver duration function of the scenario and the FEC code rate – value in italic correspond to an estimation due to simulation memory limitation**

LEO Downlink	Low complexity 10Gbit/s OOK	High complexity 25Gbit/s OOK		
FEC code	FG LDPC			
Code rate	4/5	1/2	2/3	4/5
Interleaver - number of FEC frames interleaved	6 000	6 000	9 000	<i>15 000</i>
Interleaver duration	10 ms	4 ms	6 ms	<i>10 ms</i>

## 6. CONCLUSION

In this paper, quasi cyclic LDPC codes (IRA, ARJA, FG) and Turbo Product Codes with BCH component codes have been compared to DVB-S2 (LDPC + BCH) codes. It results that FG LDPC codes achieves good performances and are an interesting alternative to current space communication standard for optical links that require low error floor and high decoder throughput. Indeed, FG LDPC codes enables decoder throughput that has not been yet obtained to the best of our knowledge for DVB-S2 codes. Very promising results are presented in [20] in which it is shown that a 10.6 Gbps decoder can be implemented into a Zynq xczu9e FPGA.

End-to-end simulations have shown the feasibility of quasi-error free communication link for both scenario with FEC code rate of 4/5 and interleaver duration around 10 ms. In future works, the two communication chains could be tested on a real time test bed.

Also, it would be interesting to compare on an identical simulation framework the performances and the hardware implementation complexity of the proposed protection schemes (FG LDPC + interleaver) with the others proposed in the literature.

## ACKNOWLEDGEMENTS

The work presented in this study was funded by CNES for the R&T DS/NT/ST-2017.0010579. We want to thank ONERA-DOTA for the fruitful discussion.

## REFERENCES

- [1] CCSDS Standardisation in Optical Communication, <https://artes.esa.int/sites/default/files/08%20-%20Klas-Juergen%20ESA.pdf>, 2017.
- [2] W. T. Roberts, S. Piazzolla, "LCRD Optical Ground Station 1", IEEE proceedings ICSOS, 2017.
- [3] H. Takenaka et al. "Study on Coding Parameters for a Small Optical Transponder", IEEE proceedings ICSOS, 2014.
- [4] S. Dimitrov et al. "Digital Modulation and Coding for Satellite Optical Feeder Links", Proceedings ASMS, 2014.
- [5] "Erasure Correcting codes for use in near Earth and deep space communication", Orange boog CCSDS, 2014.

- [6] C. Chen et al., “High-Speed Optical Links for UAV Applications”, Free Space Laser Communication LASE, 2017.
- [7] K. Ito, E. Okamoto, H. Takenata, H. Kunimori, M. Toyoshima, “Application of Polar Codes for Free Space Optical Communication”, IEEE proceedings ICSOS, 2017
- [8] H. Inoue et al. “Comparative Study on Low-Rate Forward Error Correction Codes in Downlink Satellite-to-Ground Laser Communications” IEEE proceedings ICSOS, 2014.
- [9] R. Gallager, Low density parity-check codes. IRE Trans. Inform.Theory, IT-8:pp. 2129, 1962.
- [10] Near-Optimum Decoding of Product Codes: Block Turbo Codes, R.M. Pyndiah, IEEE Transaction on communications, vol.46, No.8, 1998.
- [11] ETSI, Digital Video Broadcasting (DVB) «Second generation framing structure, channel coding and modulation systems for Broadcasting, Interactive Services, News Gathering and other broadband satellite applications; Part 1: DVB-S2DVS-S2 standard ETSI EN 302 307-1, 2014
- [12] N. Védrenne, J.-M. Conan, C. Petit, V. Michau, "Adaptive optics for high data rate satellite to ground laser link," Proc. SPIE 9739, Free-Space Laser Communication and Atmospheric Propagation XXVIII, 97390E (15 March 2016); doi: 10.1117/12.2218213
- [13] Stephen B. Alexander, [Optical Communication Receiver Design], Second Edition, 2007
- [14] T.M. Cover, J. A. Thomas, [Element of Information Theory], Second Edition, Wiley.
- [15] “AFF3CT : A Fast Forward Error Correction Toolbox,” <https://aff3ct.github.io/>.
- [16] ITU, recommendation ITU-R P.1621-1, « Propagation data required for the design of Earth-space systems operating between 20 THz and 375 THz”
- [17] M. P. C. Fossorier, “Quasicyclic low-density parity-check codes from circulant permutation matrices,” IEEE Transactions on Information Theory, vol. 50, no. 8, pp. 1788–1793, Aug 2004
- [18] W. Ryan and S. Lin, Channel Codes: Classical and Modern. Cambridge University Press, 2009
- [19] M. P. C. Fossorier, M. Mihaljevic, and H. Imai, “Reduced complexity iterative decoding of low-density parity check codes based on belief propagation,” IEEE Transactions on Communications, vol. 47, no. 5, pp. 673–680, May 1999.
- [20] V. Pignoly, B. Le Gal, C. Jegou, B. Gadat, « High data rate and flexible hardware QC-LDPC decoder for satellite optical communications”, ISTC, 2018.